Analysis and modeling of column operations on reactive dye removal onto alkaline-treated biomass fly ash

P. Pengthamkeerati[a,b,*], T. Satapanajaru[a,b]

[a]*Faculty of Environment, Department of Environmental Technology and Management, Kasetsart University, P.O. Box 1072 Kasetsart, Ngam Wong Wan Rd., Ladyaow, Chatuchak, Bangkok 10900, Thailand*
Tel. +662 942 8036; Fax: +662 942 8715; email: patthra@yahoo.com
[b]*Environmental Technology Research Unit (EnviTech), Kasetsart University, P.O. Box 1072 Kasetsart, Ngam Wong Wan Rd., Ladyaow, Chatuchak, Bangkok 10900, Thailand*

ABSTRACT

The adsorption characteristics of Reactive Black 5 (RB5) dye on alkaline-treated biomass fly ash (TFA) were investigated in aqueous solutions in a fixed-bed column. The breakthrough curves increased with decreasing initial dye concentration and the flow rate, and with increasing bed depth. In this column study, the optimum flow rate and bed depth were 5 ml min^{-1} and 10 cm, respectively. The Thomas model provided a good prediction of the breakthrough curve of RB5 removal by the TFA. The maximum adsorption capacity from the column study was in accordance with the equilibrium capacity in a batch experiment. The bed-depth service time model was used to describe the effect of bed depth on the breakthrough curves, and it revealed a good fit with the experimental data. These results suggest that the fixed-bed TFA is suitable for treating dye wastewater.

Keywords: Biomass fly ash; Alkaline treatment; Reactive dye; Fixed-bed column; Modeling

1. Introduction

A large quantity of textile wastewater is being produced in increasing amounts [1,2]. In the textile industry, reactive dye is widely used, but has a low fixation on the textile substrate, which is a cause of highly colored wastewater [3,4]. Since synthetic dye has a negative effect on the aquatic environment, e.g. reducing light penetration and photosynthesis and being toxic to aquatic life [5–8], appropriate treatment is required to treat the wastewater before it is discharged.

Adsorption is an effective method for dye removal [9]. Despite activated carbon being the most commonly used adsorbent, a number of low-cost adsorbents have been investigated for their dye removal capacity [10–13]. Among several alternative adsorbents, fly ash is of interest as a large amount is produced annually and there is a trend toward increasing quantities [14]. Previous studies have demonstrated that biomass fly ash, particularly when it has been treated with an alkaline solution, is a potential adsorbent for dye removal from wastewater [14,15] due to its greater proportion of unburned carbon that may be a substitute for commercial activated carbon.

*Corresponding author.

However, these studies determined equilibrium and kinetic parameters only in batch experiments. Further investigation in a continuous flow system is necessary for industry applications [16,17]. Since small-scale column experiments have been reported to give good predictions for dye removal from wastewater [18], they should be conducted before carrying out any high-cost, pilot-scale, column experiments.

The current study investigated the reactive dye removal from aqueous solutions on a fixed-bed column of the alkaline-treated biomass fly ash. Column adsorption performance was used to examine the effect of the initial dye concentration, flow rate, and bed depth. Mass transfer zone (MTZ) and empirical adsorption models were applied for describing the breakthrough curve behavior of dye removal.

2. Materials and methods

2.1. Fly ash and dye

The biomass fly ash was obtained from an electricity plant in eastern Thailand. The fly ash was produced from the combustion of biomass that was mainly composed of eucalypt trimmings and chips and rice husks. The sample was oven-dried at 70℃ for 24 h before use. The biomass fly ash was treated in 2 M NaOH at a solution to fly ash ratio of 15:1 by weight. The mixture was then incubated at 100℃ for 12 h. At the end of the treatment, the mixture was filtered, washed thoroughly and oven-dried at 70℃ for 24 h. The treated biomass fly ash (TFA) was then subjected to further investigation. Particle size of the TFA was analyzed by using Laser Diffraction technique (Malvern Mastersizer X, UK) and was 127 μm for mean diameter. Specific surface area (SSA) was analyzed by Autosorb-1 analyzer (Quantachrome, USA) using BET method. The TFA had a SSA of 224.13 m^2 g^{-1}. Fourier transform infrared spectroscopy (Alpha-E, Bruker) was used to identify chemical bonds and the spectrum revealed that the TFA contained groups of asymmetric Si–O–Si stretching vibration or Si–O–C structure, calcite (CaCO$_3$), symmetric Si–O–Si stretching vibration, and crystalline cristobalite, as was observed by the band intensity at a range of 900–1,250, 875, 797, and 614 cm^{-1}, respectively (Fig. 1). Chemical composition and scanning electron microscope image of the TFA were presented in the previous study [14].

The dye used in this study was Reactive Black 5 (RB5), obtained from a textile company in Thailand. RB5 is a diazo compound whose chemical structure contains anionic sulfonate groups which can be seen in Fig. 2 made available by the supplier [5].
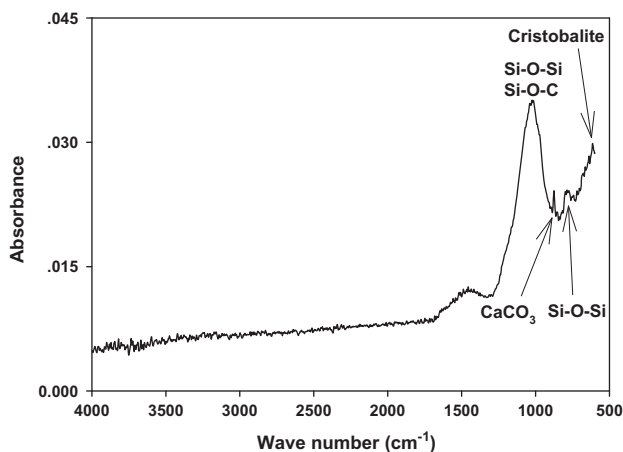
Fig. 1. FT-IR analysis of TFA.

2.2. Column study

A fixed-bed column study was conducted to investigate the capacity of the TFA for removing RB5 dye with various initial concentrations (500, 750, and 1,000 mg l^{-1}), flow rates (5, 10, and 15 ml min^{-1}), and bed heights (5, 7.5, and 10 cm) under continuous flow conditions. A plexiglass column of 2.54 cm diameter and 50 cm height was filled with the TFA. The column was loaded with dye solution which flowed upward using a peristaltic pump. The dye concentration in the effluent solution was periodically measured by using a UV–vis spectrophotometer (UV-1700 PharmaSpec model, Shimadzu) at λ_{max} of 598 nm. The column operation was terminated when more than 90% of the capacity was used up.

2.3. Mathematical expressions and models for adsorption

2.3.1. MTZ

The breakthrough curve is typically plotted between C/C_0 (C and C_0 = concentration at a given time t and the initial concentration, respectively) and the treated volume. In a fixed-bed column, the MTZ is the portion of the breakthrough curve between the effluent concentration at exhaustion (C_E) and the concentration at the breakthrough point (C_b) which is assumed to have a constant depth. C_b and C_E in this study corresponded to $C/C_0 = 0.005$ and 0.90, respectively. The following equations were obtained from Michaels [19] and Kundu and Gupta [20]. The time (t_z) required for the MTZ to move its own height down through the bed once it has been established (min) is calculated from Eq. (1).

$$t_z = V_z/Q = (V_E - V_b)/Q \qquad (1)$$
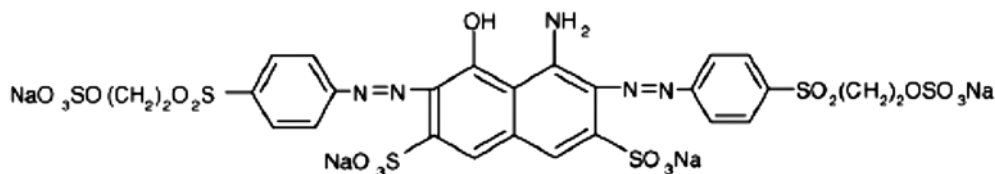
Fig. 2. Chemical structure of RB5 dye.

where V_z = volume of effluent between breakthrough and exhaustion (ml) and Q = influent flow rate (ml min^{-1}).

The time (t_E) required for the MTZ to become established and move completely out of the bed is calculated from Eq. (2).

$$t_E = V_E/Q \tag{2}$$

where V_E = total volume of effluent to the point of exhaustion.

The height of the MTZ (h_z) and the rate (U_z) of movement of the MTZ up or down through the bed (cm h^{-1}) are determined from Eqs. (3) and (4), respectively.

$$h_z = h(t_z)/(t_E - t_f) \tag{3}$$

$$U_z = h_z/t_z = h/(t_E - t_f) \tag{4}$$

where h = total bed depth (cm); and t_f = time (min) required for the MTZ to initially form, calculated from Eq. (5).

$$t_f = (1 - f)t_z \tag{5}$$

The fraction (f) of the adsorbent present in the MTZ still possessing the ability to remove the RB5 dye is calculated as follows.

$$f = q_z/q_{max} = \int_{V_b}^{V_E} (C_0 - C)dV/C_0 V_z \tag{6}$$

where q_z and q_{max} = amount of adsorbate that has been removed by the MTZ from breakthrough to exhaustion and if completely exhausted, respectively.

2.3.2. Maximum capacity of column (q_e)

In column study, q_e is defined by Eq. (7) as the total amount of adsorbed (q_{total}) per unit weight of adsorbent (w) at the end of total flow time [21]. q_{total} is equal to the area under the breakthrough curve obtained by integrating the adsorbed concentration ($C_{ad} = C_0 - C_t$: mg l^{-1}) vs. time (t: min) plot and is defined by Eq. (8) [21].

$$q_e = q_{total}/w \tag{7}$$

$$q_{total} = \left(Q \int_{t=0}^{t=t_{total}} C_{ad}\,dt \right) \Big/ 1000 \tag{8}$$

where t_{total} = total flow time (min) up to the column exhaustion point for this study.

2.3.3. Thomas model

The Thomas model is widely used to characterize the breakthrough curve in a system with a constant flow rate and no axial dispersion, and its behavior matches the Langmuir isotherms and the second-order kinetics [22]. The model is based on Eq. (9).

$$C/C_0 = 1/(1 + \exp[(k_{Th}/F)(q\,m - C_0 V)]) \tag{9}$$

where k_{Th} = rate constant (l g^{-1} h^{-1}); F = linear flow velocity (cm min^{-1}); q = adsorption capacity (mg g^{-1}); and m = mass of the bed (g).

2.3.4. Bed-depth service time (BDST)

A modification of the Bohart–Adams equation by Hutchins [20] is known as the BDST model. The BDST model is based on a linear relationship between the bed depth or bed height (h) and the service time (t) as shown in Eq. (10).

$$t = (N_0 h)/(C_0 F) - (1/(C_0 K))(\ln (C_0/C_b - 1)) \tag{10}$$

where N_0 = adsorption capacity (mg l^{-1}); and K = adsorption rate constant (L mg^{-1} min^{-1}).

3. Results and discussion

3.1. Effect of initial dye concentration

The breakthrough curves of the RB5 removal by the TFA at different initial dye concentrations (C_0) are shown in Fig. 3. The column adsorption parameters are given in Table 1. As expected, higher C_0 values gave earlier breakthrough curves, and the breakthrough time (V_b) and exhaustion time (V_E) decreased when C_0 increased from 500 to 1,000 mg l^{-1} for both the studied flow rates. This indicated that a better column performance was provided at lower C_0 perhaps because the competition for adsorption was less at lower C_0 and, therefore, a larger treated volume was obtained. On the other hand, the TFA was becoming exhausted faster at higher C_0, due to the higher mass of dye molecules per unit area on the TFA surface.
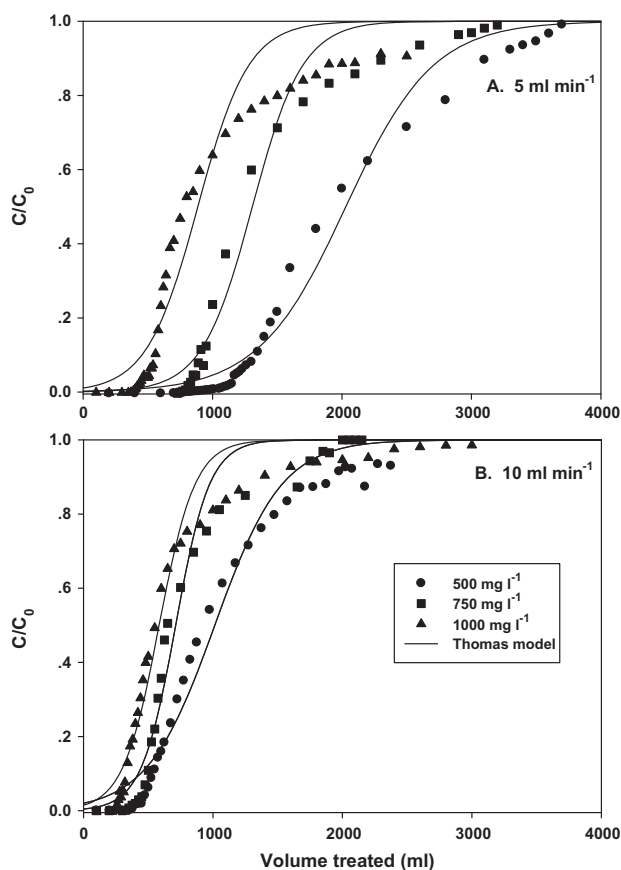
Fig. 3. Effect of initial dye concentration on the breakthrough curves of RB5 removal by the alkaline-treated biomass fly ash at the flow rate of (A) 5 ml min^{-1} and (B) 10 ml min^{-1}. Experimental conditions: initial dye concentration range of 500, 750, and 1,000 mg l^{-1}; bed depth of 10 cm. Points: experimental data, lines: predicted data from the Thomas model.

In addition, the height of the MTZ (h_z) and the rate (U_z) of movement of the MTZ decreased with decreasing C_0. h_z determined the adsorption rate by the adsorbent and gives indications about the diffusion resistance [23]. Theoretically, the shorter h_z is the faster rate of adsorption and the lower resistance to the mass transfer [23,24]. U_z is used to calculate the rate of bed saturation, and is directly related to h_z [23]. The smaller h_z is the faster rates of mass transfer and bed saturation. According to the h_z and U_z values obtained from this study, a higher column performance was provided at lower C_0. Al-Degs et al. [18] investigated the column adsorption characteristics of RB5 by granular activated carbon and also observed a decreased h_z and U_z with lowering C_0. In this present study, h_z was higher than the bed depth used. This observation indicated that the TFA column gave a high diffusion resistance to the mass transfer, possibly because the TFA particles were relatively small with a mean particle diameter of 127 μm. Similar observation was also reported by Rivera-Utrilla et al. [25] and Ahamad and Jawed [26], who observed the higher h_z than the bed depth when using activated carbon and wooden charcoal and sand, respectively, as an adsorbent for metals.

Column adsorption capacities (q_e) obtained from the column experiments had a tendency to increase with an increased C_0 for both the flow rates studied (Table 1). This is because the concentration gradient across the fluid film surrounding the adsorbent particle was higher at higher C_0 [27]. Hence, more adsorption sites were being covered as the C_0 increases [28], resulting in better dye adsorption. This finding was in agreement with the studies by Al-Degs et al. [18] and Vijayaraghavan and Yun [29], who reported that the adsorption capacities for RB5 removal in the column study were increased from 36 to 107 and 88.9 to 103.2 mg g^{-1} with C_0, respectively.

The theoretical breakthrough curves calculated using the Thomas model are shown in Fig. 3 and the model parameters are shown in Table 1. The regression coefficient indicated that the Thomas model ($r^2 = 0.93$–0.98) was a good fit with the experimental data. The good agreement with the Thomas model indicated that the adsorption behavior of the TFA fits the Langmuir isotherm and second-order kinetic models [22], as was found in the batch experiment [14]. The value k_{th} is the rate constant that characterizes the rate of solute transfer from the liquid to the solid phase, and the higher the value of k_{th}, the greater the kinetically favorable adsorption [17]. Except for 750 mg l^{-1} at a rate of 10 ml min^{-1}, the calculated k_{th} value was not much different among the different C_0 values applied in this study, indicating similar kinetically

Table 1
Influence of experimental conditions on column adsorption parameters of RB5 on the alkaline-treated biomass fly ash and the parameters of Thomas model using nonlinear regression analysis

Initial dye concentration (mg l^{-1})	Flow rate (ml min^{-1})	Bed depth (cm)	MTZ parameters					Thomas model		
			V_b (ml)	V_E (ml)	h_z (cm)	U_z (cm h^{-1})	$q_{e,\ column}$[a] (mg g^{-1})	k_{th} (l g^{-1} h^{-1})	q_{model}[b] (mg g^{-1})	r^2
500	5	10	963	3,131	10.5	1.5	98.24	1.77	96.66	0.98
750	5	10	785	2,338	11.3	2.2	97.90	2.06	93.44	0.98
1,000	5	10	394	2,201	17.8	3.0	107.91	1.53	94.09	0.93
500	10	10	377	1,931	14.8	5.7	58.53	4.60	56.65	0.97
750	10	10	341	1,688	16.4	7.3	63.79	6.07	55.38	0.97
1,000	10	10	245	1,380	17.1	9.1	63.63	4.32	56.20	0.97
1,000	5	10	394	2,201	17.8	3.0	107.91	1.53	94.09	0.93
1,000	10	10	245	1,380	17.1	9.1	63.63	4.32	56.20	0.97
1,000	15	10	214	1,393	21.6	16.5	51.91	8.70	42.19	0.95
1,000	5	5	101	1,176	12.1	3.4	91.35	2.80	74.27	0.92
1,000	5	7.5	215	1,737	15.7	3.1	100.11	2.03	84.33	0.95
1,000	5	10	394	2,201	17.8	3.0	107.91	1.53	94.09	0.93

[a]$q_{e,\ column}$ = maximum adsorption capacity obtained from the experimental data.
[b]q_{model} = maximum adsorption capacity calculated from the Thomas model.

favorable conditions. For all C_0 values, the adsorption capacities from the model (q_{model}) were in the same ranges of 93.44–96.66 and 55.38–56.65 mg g^{-1} for the flow rates of 5 and 10 cm min^{-1}, respectively. For each flow rate studied, the obtained q_{model} was in a similar range with the q_e from the experiment (Table 1).

3.2. Effect of flow rate

In a continuous system, the flow rate is an important parameter influencing the performance of the adsorbent [17]. Figs. 3 and 4(a) show the breakthrough curves for different flow rates at the C_0 value of 1,000 mg l^{-1} and a bed height of 10 cm. The adsorption parameters of the column are given in Table 1. With an increased flow rate, the breakthrough curves had a steeper slope and a shift to the origin, as was mostly found with lower V_b and V_E values for a higher flow rate. This indicated that the column was exhausted faster with a higher flow rate, possibly leading to less saturation of the TFA. With high flow rate, the solute in the solution might have a lower contact time or insufficient time to penetrate to and react with the adsorption sites, resulting in a shorter breakthrough time and improper utilization of the adsorption capacity [29]. The h_z and U_z values decreased with a decreased flow rate. Since a short h_z indicates a high adsorption rate, the lower flow rate used in this study had a higher adsorption rate, except for when C_0 was

1,000 mg l^{-1} when the 5 and 10 ml min^{-1} flow rates had similar h_z values.

In this study, there was good agreement between the experimental data and the predicted data from the Thomas model (Table 1). The q_e values from the experiment and the q_{model} values decreased with an increase in the flow rate from 5 to 15 ml min^{-1} (Table 1). This observation was in agreement with the relevant studies on RB5 removal by Ahmad and Hameed [21] and Vijay-araghavan and Yun [29]. From the Thomas model, the calculated k_{th} value increased with the flow rate (Table 1), and the higher k_{th} value for the increased flow rates suggested more kinetically favorable adsorption which possibly was due to an increase in the rate of mass transfer at the higher flow rate [21].

For the lowest flow rate studied (5 ml min^{-1}), the adsorption capacities were the highest in this column study (Table 1) and were close to the maximum equilibrium capacities of the Langmuir and second-order kinetic models (107.53 and 97.09 mg g^{-1}, respectively) [14]. This indicated that the adsorption capacity of the TFA was almost fully utilized at this flow rate. Hence, this flow rate was appropriate for dye removal under the studied experimental conditions.

3.3. Effect of bed depth

Fig. 4(b) and Table 1 show the effect of bed depth on the breakthrough curve of RB5 removal at the C_0
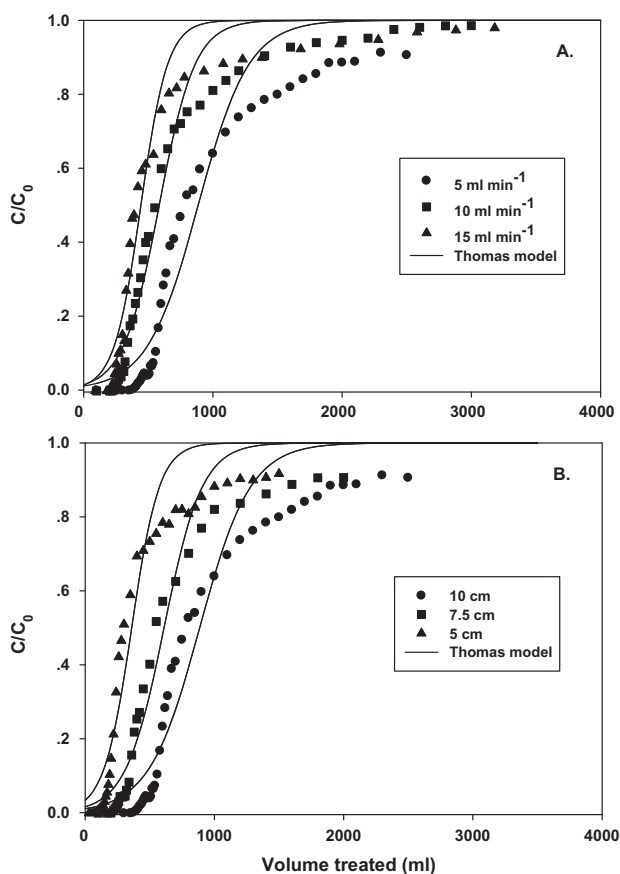
Fig. 4. Effect of (A) flow rate and (B) bed depth on the breakthrough curves of RB5 removal by the alkaline-treated biomass fly ash. Experimental conditions: (A) flow rate of 5, 10 and 15 ml min^{-1}; initial concentration (C_0) of 1,000 mg l^{-1}; bed depth at 10 cm, and (B) flow rate of 5 ml min^{-1}; $C_0 = 1,000$ mg l^{-1}; bed depth of 5, 7.5 and 10 cm. Points: experimental data, lines: predicted data from the Thomas model.

value of 1,000 mg l^{-1} and a flow rate of 5 ml min^{-1}. All the studied bed depths gave a similar shaped break-through curve, with a slightly flatter slope as the bed depth increased, suggesting that the adsorption rates were not considerably different among the bed depths [24]. An increased bed depth (or sorbent mass) provided a greater surface area for dye adsorption and increased the contact time between the bed and the dye [16]. As expected, the V_b and V_E values increased with a higher bed depth in this study. In addition, both the q_e values obtained from the experimental data and the q_{model} values from the Thomas model increased with increasing bed depth. A similar result was also reported by Ahmad and Hameed [21] and Vijayaraghavan and Yun [29] that the bed capacities of RB5 removal by waste-based activate carbon and

biosorbent, respectively, increased with increasing bed depth. Despite the relatively high r^2 values (0.92–0.95) were obtained from fitting the Thomas model to the experimental data in this bed-depth study, the q_{model} values were quite lower than the q_e from the experiments. This might be because the breakthrough curves for each bed depth did not reach the C/C_0 of 1, indicating mass transfer limitation of the system. Similar observation was reported by Sekhula et al. [30], who found high r^2 values of the Thomas model ($r^2 = 0.97–0.98$), but some of the breakthrough curves did not reach the C/C_0 of 1. Also, Salmani et al. [31] observed high r^2 values of the Thomas model ($r^2 = 0.98$), despite the breakthrough curves did not reach the C/C_0 of 1.

The highest adsorption capacity at 10 cm bed depth was close to the maximum equilibrium capacity [14], indicating a sufficient contact time between the bed and the dye. The k_{th} value increased with decreasing bed depth, but was not considerable in comparison with the effect of the flow rate. In this study, an increased bed depth of the TFA (up to 10 cm) might be important in obtaining a better column performance for RB5 removal.

Increasing the bed depth increased h_z (Table 1), possibly due to creating a longer distance for the MTZ to reach the exit [32]. In addition, the increase in h_z with bed depth suggested that the reactive dye had slow adsorption kinetics on the bed, resulting in an increased adsorption zone at higher bed depth [18]. Interestingly, U_z was not different among the studied bed depths (Table 1), reflecting the same affinity of RB5 for the TFA.
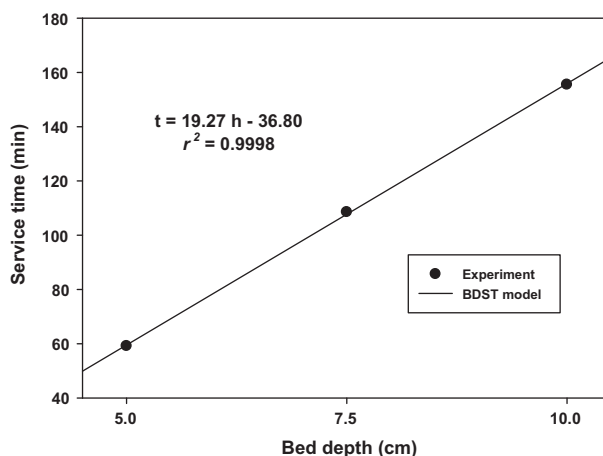
Fig. 5. Relationship between bed depth and service time at 50% saturation for the RB5 removal by the alkaline-treated biomass fly ash (flow rate of 5 ml min^{-1} and initial concentration (C_0) of 1,000 mg l^{-1}). Points: experimental data, lines: predicted data from the BDST model.

The adsorption data of RB5 by the TFA at different bed depths was analyzed using the BDST model (Fig. 5). The regression equation between the bed depth and service time for 50% saturation ($C/C_0 = 0.5$) of the TFA column was $t = 19.27h - 36.80$ ($r^2 = 0.9998$). The fact that the BDST line does not pass through the origin suggests that more than one rate-limiting step could be involved in the adsorption process [17,18]. The BDST adsorption capacity (N_0) obtained from Eq. (10) was 19,006 mg l^{-1} or 100.45 mg g^{-1}. The calculated N_0 is consistent with the adsorption capacities from the experimental data and the Thomas model at the bed depth of 10 cm (Table 1) and the maximum equilibrium capacity from the batch experiment [14]. The highest adsorption capacity of RB5 in the current study was in agreement with those values sourced from the literature. For example, Ahmad and Hameed [21] found that a column of granular activated carbon prepared from bamboo waste had the highest bed capacity of 39.09 mg g^{-1} for RB5 removal. Al-Degs et al. [18] showed that the highest column capacity of RB5 adsorption using commercial activated carbon (Filtrasorb 400) was 107 mg g^{-1}. In addition, Vijayaraghavan and Yun [29] observed the highest adsorption capacity of 103.2 mg g^{-1} for RB5 removal by biosorbent. These results proved that the TFA was an effective dye adsorbent that could be substituted for activated carbon.

4. Conclusions

The breakthrough curves of the RB5 dye removal by the TFA increased with decreasing the initial dye concentration and flow rate, and with increasing the bed depth. The experimental breakthrough curve was in accordance with the predicted curve from the Thomas model. In this fixed-bed column study, the optimum flow rate and bed depth were 5 ml min^{-1} and 10 cm, respectively. Regardless of the initial dye concentrations, this flow rate and bed depth provided the highest efficiency for dye adsorption that was close to the equilibrium capacity from the batch experiment. The effect of the bed depth on the breakthrough curve was well explained by the BDST model. These findings show that the fixed-bed TFA has potential for application in the removal of reactive dye.

References

[1] S.K. Alpat, Ö. Özbayrak, Ş. Alpat, H. Akçay, The adsorption kinetics and removal of cationic dye, Toluidine Blue O, from aqueous solution with Turkish zeolite, J. Hazard. Mater. 151 (2008) 213–220.

[2] R. Gong, Y. Ding, M. Li, C. Yang, H. Liu, Y. Sun, Utilization of powdered peanut hull as biosorbent for removal of anionic dyes from aqueous solution, Dyes Pigm. 64 (2005) 187–192.

[3] J.J.M. Órfão, A.I.M. Silva, J.C.V. Pereira, S.A. Barata, I.M. Foseca, P.C.C. Faria, M.F.R. Pereira, Adsorption of a reactive dye on chemically modified activated carbons-influence of pH, J. Colloid Interface Sci. 296 (2006) 480–489.

[4] Y.S. Aldegs, M.I. Elbarghouthi, A.H. Elsheikh, G.M. Walker, Effect of solution pH, ionic strength, and temperature on adsorption behavior of reactive dyes on activated carbon, Dyes Pigm. 77 (2008) 16–23.

[5] A. Aguedach, S. Brosillon, J. Morvan, E.K. Lhadi, Photocatalytic degradation of azo-dyes reactive black 5 and reactive yellow 145 in water over a newly deposited titanium dioxide, Appl. Catal., B 57 (2005) 55–62.

[6] A.R. Dincer, Y. Gunes, N. Karakaya, E. Gunes, Comparison of activated carbon and bottom ash for removal of reactive dye from aqueous solution, Biore-sour. Technol. 98 (2007) 834–839.

[7] V.S. Mane, I.D. Mall, V.C. Srivastava, Kinetic and equilibrium isotherm studies for the adsorptive removal of Brilliant Green dye from aqueous solution by rice husk ash, J. Environ. Manage. 84 (2007) 390–400.

[8] V. Ponnusami, V. Krithika, R. Madhuram, S.N. Srivastava, Biosorption of reactive dye using acid-treated rice husk: Factorial design analysis, J. Hazard. Mater. 142 (2007) 397–403.

[9] P.C.C. Faria, J.J.M. Órfão, M.F.R. Pereira, Adsorption of anionic and cationic dyes on activated carbons with different surface chemistries, Water Res. 38 (2004) 2043–2052.

[10] A. Bousher, X. Shen, R.G.J. Edyvean, Removal of coloured organic matter by adsorption onto low-cost waste materials, Water Res. 31 (1997) 2084–2092.

[11] P. Janos, H. Buchtova, M. Ryznarova, Sorption of dyes from aqueous solutions onto fly ash, Water Res. 37 (2003) 4938–4944.

[12] M. Özacar, İ.A. Şengil, Adsorption of reactive dyes on calcined alunite from aqueous solutions, J. Hazard. Mater. 98 (2003) 211–224.

[13] S. Wang, Z.H. Zhu, Sonochemical treatment of fly ash for dye removal from wastewater, J. Hazard. Mater. 126 (2005) 91–95.

[14] P. Pengthamkeerati, T. Satapanajaru, N. Chatsatapattayakul, P. Chairattanamanokorn, N. Sananwai, Alkaline treatment of biomass fly ash for reactive dye removal from aqueous solution, Desalination 261 (2010) 34–40.

[15] P. Pengthamkeerati, T. Satapanajaru, O. Singchan, Sorption of reactive dye from aqueous solution on biomass fly ash, J. Hazard. Mater. 153 (2008) 1149–1156.

[16] J. Barron-Zambrano, A. Szygula, M. Ruiz, A.M. Sastre, E. Guibal, Biosorption of Reactive black 5 from aqueous solutions by chitosan: Column studies, J. Environ. Manage. 91 (2010) 2669–2675.

[17] M. Lezehari, M. Baudu, O. Bouras, J-P. Basly, Fixed-bed column studies of pentachlorophenol removal by use of alginate-encapsulated pillared clay microbeads, J. Colloid Interface Sci. 379 (2012) 101–106.

[18] Y.S. Al-Degs, M.A.M. Khraisheh, S.J. Allen, M.N. Ahmad, Adsorption characteristics of reactive dyes in columns of activated carbon, J. Hazard. Mater. 165 (2009) 944–949.

[19] A.S. Michaels, Simplified method of interpreting kinetic data in fixed-bed ion exchange, Ind. Eng. Chem. 44 (1952) 1922–1930.

[20] S. Kundu, A.K. Gupta, Analysis and modeling of fixed bed column operations on As(V) removal by adsorption onto iron oxide-coated cement (IOCC), J. Colloid Interface Sci. 290 (2005) 52–60.

[21] A.A. Ahmad, B.H. Hameed, Fixed-bed adsorption of reactive azo dye onto granular activated carbon prepared from waste, J. Hazard. Mater. 175 (2010) 298–303.

[22] M. Trgo, N.V. Medvidovic, J. Peric, Application of mathematical empirical models to dynamic removal of lead on natural zeolite clinoptilolite in a fixed bed column, Indian J. Chem. Technol. 18 (2011) 123–131.

[23] N. Hanen, O. Abdelmottaleb, Modeling of the dynamics adsorption of phenol from an aqueous solution on activated carbon produced from olive stones, J. Chem. Eng. Process Technol. 4 (3) (2013) 1–7.

[24] D. Inthorn, K. Tipprasertsin, P. Thiravetyan, E. Khan, Color removal from textile wastewater by using treated flute reed in a fixed bed column, J. Environ. Sci. Health., Part A 45 (2010) 637–644.

[25] J. Rivera-Utrilla, I. Bautista-Toledo, M.A. Ferro-García, C. Moreno-Castilla, Bioadsorption of Pb(II), Cd(II), and Cr(VI) on activated carbon from aqueous solutions, Carbon 41 (2003) 323–330.

[26] K.U. Ahamad, M. Jawed, Breakthrough column studies for iron(II) removal from water by wooden charcoal and sand: A low cost approach, Int. J. Environ. Res. 5 (2011) 127–138.

[27] S. Singh, M.K.N. Yenkie, Adsorption of o-cresol from its aqueous solution on granular activated carbon columns, Asian J. Chem. 13 (2001) 1349–1362.

[28] R. Han, Y. Wang, X. Zhao, Y. Wang, F. Xie, J. Cheng, M. Tang, Adsorption of methylene blue by phoenix tree leaf powder in a fixed-bed column: Experiments and prediction of breakthrough curves, Desalination 245 (2009) 284–297.

[29] K. Vijayaraghavan, Y-S. Yun, Polysulfone-immobilized Corynebacterium glutamicum: A biosorbent for Reactive black 5 from aqueous solution in an up-flow packed column, Chem. Eng. J. 145 (2008) 44–49.

[30] M.M. Sekhula, J.O. Okonkwo, C.M. Zvinowanda, N.N. Agyei, A.J. Chaudhary, Fixed bed column adsorption of Cu(II) onto maize tassel-PVA beads, J. Chem. Eng. Process Technol. 3 (131) (2012) 1–5.

[31] M.H. Salmani, M. Vakili, M.H. Ehrampoush, A comparative study of copper (ii) removal on iron oxide, aluminum oxide and activated carbon by continuous down flow method, J. Toxicol. Environ. Health Sci. 5 (2013) 150–155.

[32] Z.Z. Chowdhury, S.M. Zain, A.K. Rashid, R.F. Rafique, K. Khalid, Breakthrough curve analysis for column dynamics sorption of Mn(II) ions from wastewater by using Mangostana garcinia peel-based granular-activated carbon, J. Chem. 2013 (2013) 1–8, doi: 10.1155/2013/959761